

Coordination of a mitochondrial superoxide burst during the hypersensitive response to bacterial pathogen in *Nicotiana tabacum*

MARINA CVETKOVSKA^{1,2} & GREG C. VANLERBERGHE^{1,2}

¹Department of Biological Sciences and ²Department of Cell and Systems Biology, University of Toronto Scarborough, Toronto, Ontario, Canada M1C 1A4

ABSTRACT

We characterized responses of *Nicotiana tabacum* to pathovars of the bacterial pathogen *Pseudomonas syringae*. These included a compatible response associated with necrotic cell death (*pv. tabaci*), an incompatible response that included hypersensitive response (HR) cell death (*pv. maculicola*) and an incompatible response that induced defences but lacked the HR (*pv. phaseolicola*). Signalling molecules (salicylic acid, nitric oxide, H₂O₂) known to induce the stress responsive tobacco *Aox1a* gene [that encodes the mitochondrial electron transport chain (ETC) component alternative oxidase (AOX)] accumulated preferentially during the HR, but this did not elevate *Aox1a* transcript or AOX protein, while the transcript and protein were strongly elevated during the defence response to *pv. phaseolicola*. In addition, matrix manganese superoxide dismutase (MnSOD) activity declined during the HR, unlike its response to the other pathovars, and unlike the response of other superoxide dismutase (SOD) enzymes. Finally, the HR (but not the response to *pv. phaseolicola* or *pv. tabaci*) was accompanied by an early and persistent mitochondrial superoxide (O₂⁻) burst prior to cell death. We propose that a coordinated response of the major ETC mechanism to avoid O₂⁻ generation (AOX) and the sole enzymatic means to scavenge mitochondrial O₂⁻ (MnSOD) is important in the determination of cell fate during responses to pathogen.

Key-words: alternative oxidase; manganese superoxide dismutase; mitochondrion; nitric oxide; programmed cell death; *Pseudomonas syringae*; salicylic acid; superoxide; tobacco.

Abbreviations: ACC oxidase, 1-aminocyclopropane-1-carboxylic acid oxidase; AOX, alternative oxidase; CuZnSOD, copper zinc superoxide dismutase; cyt, cytochrome; ETC, electron transport chain; FeSOD, iron superoxide dismutase; HR, hypersensitive response; MnSOD, manganese superoxide dismutase; NO, nitric oxide; O₂⁻, superoxide; ONOO⁻, peroxynitrite; PCD, programmed cell

death; *PR-I*, pathogenesis-related-1; PVP, polyvinylpyrrolidone; ROS, reactive oxygen species; SA, salicylic acid; SAG, salicylic acid β-glucoside; SOD, superoxide dismutase.

INTRODUCTION

Infection of a plant by a pathogen has two possible outcomes – disease (compatible interaction) or resistance (incompatible interaction). During one type of incompatible interaction, recognition of the pathogen by the plant triggers the HR, a localized PCD thought to delay pathogen spread (Coll, Eppie & Dangl 2011). Even though this host-controlled process may not be essential for resistance, it is required for the rapid and strong activation of other defence responses (Heath 2000). Another type of incompatible interaction occurs if the pathogen fails to overcome even basal defence barriers and fails to proliferate. While such an interaction does not induce the HR, it does nonetheless induce other defence responses (Mysore & Ryu 2004). In a typical compatible interaction, the pathogen is able to suppress or overcome basal and induced plant defences, thus successfully colonizing the host and causing disease (Nomura, Melotto & He 2005).

Recent research has established that the mitochondrion is likely an important player in plant PCD, including the HR, although the details of its role are not well understood and expected to differ from that seen in animals (Lam, Kato & Lawton 2001; Amirsadeghi, Robson & Vanlerberghe 2007; Noctor, De Paepe & Foyer 2007; van Doorn *et al.* 2011). An important emerging theme, however, is that the mitochondrion may be an important early source of intracellular ROS, a so-called mitochondrial oxidative burst. This is accompanied by changes in mitochondrial membrane potential, the mitochondrial permeability transition, cyt *c* release (at least in some cases) and changes in mitochondrial morphology (Arpagaus, Rawlyer & Braendle 2002; Tiwari, Belenghi & Levine 2002; Yao *et al.* 2002, 2004; Weir, Pham & Hedley 2003; Takahashi *et al.* 2004; Ashtamker *et al.* 2007; Garmier *et al.* 2007). In some cases, blockage of one or more of these events, such as inhibition of the permeability transition by cyclosporine A, is shown to block or delay PCD. Nonetheless, it remains obscure what overall role and influence these mitochondrial events have in PCD.

Correspondence: G. C. Vanlerberghe. E-mail: gregv@utsc.utoronto.ca

Besides cytochrome oxidase, plants have an additional terminal oxidase in the mitochondrial ETC called AOX that catalyses the oxidation of ubiquinol and reduction of O_2 to H_2O , and which has been linked to the control of ROS generation by the ETC (Finnegan, Soole & Umbach 2004; Vanlerberghe, Cvetkovska & Wang 2009). AOX is non-proton pumping and since it bypasses proton-pumping complexes III and IV, electron flow to AOX dramatically reduces the energy yield of respiration. AOX is encoded by a small nuclear gene family and is an interfacial membrane protein on the matrix side of the inner membrane. Many AOX members contain a conserved regulatory Cys residue that confers tight biochemical control, linking AOX activity to prevailing metabolic conditions. Because of its non-energy conserving nature, AOX reduces the otherwise tight coupling between carbon metabolism, electron transport and ATP turnover. This flexibility in metabolism is likely important in numerous contexts, but particularly under stress conditions (Finnegan *et al.* 2004; Vanlerberghe *et al.* 2009). A central hypothesis is that AOX acts to dampen O_2^- generation by the ETC, since it bypasses Complex III, an important source of O_2^- , and since its energy-dissipating nature will act to moderate membrane potential. This will lower the overall reduction state of ETC components, lessening the electron leak that produces O_2^- (Møller 2001). Supporting this, chemical inhibition of AOX or assay conditions that do not favour the activation of AOX result in higher rates of ROS generation by isolated mitochondria (Purvis 1997; Braidot *et al.* 1999). Furthermore, in transgenic tobacco suspension cells, silencing of AOX was accompanied by increased ROS that appeared to emanate specifically from the mitochondria (Maxwell, Wang & McIntosh 1999).

SA, NO and ROS such as H_2O_2 and O_2^- are important signalling molecules to initiate and coordinate defence responses, including the HR, during incompatible interactions (Leitner *et al.* 2009; Vlot, Dempsey & Klessig 2009; Spoel & Loake 2011). Interestingly, strong links exist between these signalling molecules and mitochondria. A low level of exogenously applied SA can disrupt the ETC, although the mechanism(s) involved is poorly understood (Norman *et al.* 2004; de Souza *et al.* 2011). Perhaps due to this disruption, SA dramatically induces the level of AOX transcript and protein in many species (Rhoads & McIntosh 1992; Van Der Straeten *et al.* 1995; Ho *et al.* 2008). NO is a well-known competitive inhibitor of cytochrome oxidase, but AOX is not subject to this inhibition (Millar & Day 1996), and exogenous applied NO has been demonstrated to be an effective inducer of AOX gene expression (Huang, von-Rad & Durner 2002; Ederli *et al.* 2006). What is not clear is whether the ability of NO to induce AOX results primarily from it acting as a respiratory inhibitor or whether NO can also induce AOX through its action as a signalling molecule, independent of inhibition of cytochrome oxidase. O_2^- is a well-established by-product of ETC activity and, once produced, can be scavenged and converted to H_2O_2 by a mitochondrion-specific and matrix-localized MnSOD (Møller 2001). Finally, exogenous H_2O_2 can induce AOX gene expression (Vanlerberghe & McIntosh 1996), and

H_2O_2 -responsive elements are present in the stress-responsive *Aox1a* gene of *Arabidopsis* (Ho *et al.* 2008).

Disparate studies have investigated the role of mitochondrial ROS in PCD, the role of AOX in avoiding ROS generation and links between mitochondrial function and biotic stress signalling molecules. Based on these studies, we proposed that AOX might be an important determinant of cell fate during responses to pathogens. To robustly test this hypothesis, we characterized the response of *Nicotiana tabacum* to pathovars of *Pseudomonas syringae*. Based on our results, we propose that a coordinated response of the major ETC mechanism to avoid O_2^- generation (AOX) and the sole enzymatic means to scavenge mitochondrial O_2^- (MnSOD) is important in the determination of cell fate during responses to pathogen.

MATERIALS AND METHODS

Plant material and growth conditions

N. tabacum L. cv. Petit Havana SR1 was grown in controlled-environment chambers (PGR-15, Conviron, Winnipeg, Canada) with a 16 h photoperiod, temperature of 28 °C/22 °C (light/dark), relative humidity of 60%, photosynthetic photon flux density of 130 $\mu\text{mol m}^{-2} \text{s}^{-1}$, and in a general-purpose growing medium (Pro-mix BX, Premier Horticulture, Canada). Plants were irrigated with water daily and fertilized with 10× diluted Hoagland's solution three times per week. *Arabidopsis thaliana* ecotype Columbia was grown similarly but with a 9 h photoperiod, constant temperature (22 °C), relative humidity of 65% and photosynthetic photon flux density of 200 $\mu\text{mol m}^{-2} \text{s}^{-1}$. Plants were grown in the same medium as above and irrigation alternated between water and general-purpose fertilizer (Plant Products, Brampton, Canada). Plants were used 5–6 weeks after initiating germination in vermiculite (tobacco) or soil (*Arabidopsis*). Tobacco suspension cells were derived from leaf tissue and grown heterotrophically as previously described (Robson & Vanlerberghe 2002). Cultures were maintained in the dark on a rotary shaker (140 rpm, 28 °C) and were subcultured every 7 days by dilution in fresh growth medium. Cells (200 mL cultures) were used at 2 days after subculture.

Bacteria and plant inoculations

P. syringae pv. *tabaci*, pv. *maculicola* ES4326, pv. *phaseolicola* NPS3121 and pv. *tomato* strains DC3000, DC3000 (*avrRpt2*) and DC3000 (*avrRps4*) were each acquired from Dr K. Yoshioka, University of Toronto. All bacteria were cultured in King's B medium (King, Ward & Raney 1954), either without antibiotic (pv. *maculicola*), with 50 $\mu\text{g mL}^{-1}$ rifamycin (pv. *phaseolicola*), or with 50 $\mu\text{g mL}^{-1}$ each of kanamycin and rifamycin (pv. *tabaci* and pv. *tomato*). Bacteria were grown overnight with rotation (28 °C, ~20 rpm), washed once and resuspended in distilled water (for tobacco) or 10 mM MgCl_2 (for *Arabidopsis*). Culture density was determined by absorbance at 600 nm using a

spectrophotometer (HP8452, Agilent Technologies, Mississauga, Canada). Unless stated otherwise, density was adjusted to 1×10^7 cfu mL⁻¹ for plant inoculations, care being taken to inoculate comparable leaves between plants. Tobacco were inoculated at 5 h into the light period by completely infiltrating with liquid the abaxial side of the second to lowest true leaf, using a syringe with needle. Mock-inoculated plants were infiltrated with distilled water. *Arabidopsis* were inoculated at 1 h into the light period by completely infiltrating the abaxial side of rosette leaves using a syringe without needle. Mock inoculations were carried out with 10 mM MgCl₂.

Bacterial growth *in planta* and leaf cell death

Bacterial growth *in planta* was determined by harvesting three leaf discs (1 cm diameter), homogenizing in 10 mM MgCl₂, and plating as a dilution series on King's B medium agar plates supplemented with the appropriate antibiotics. Following incubation (2 d, 28 °C), the number of bacterial colonies was determined. The symptoms of the infection were assessed and compared visually, while leaf cell death was also measured using an ion leakage assay. Ten leaf discs (1 cm diameter) were floated abaxial side up on 10 mL distilled water for 4 h in the dark at room temperature (RT). After incubation, conductivity of the bathing solution was measured with a conductivity meter (CON510, Oakton Instruments, Vernon Hills, IL, USA).

SA determination

Measurement of SA levels was done according to the method of Mosher *et al.* (2010), with some modifications. Leaf tissue (0.1 g FW) was flash frozen in liquid N₂ and extracted twice with 0.8 mL extraction buffer {acetone: 50 mM citric acid [70:30] and 5 µL of internal standard [²H₆SA; CDN isotopes, Point-Claire, Quebec, Canada]} in 1.5 mL screw-cap tubes containing 1.4 mm ceramic beads (Qbiogene, Carlsbad, CA, USA) and using a FastPrep FP120 homogenizer (Qbiogene). After centrifugation (14 000 g, 3 min, RT), the supernatant was removed to a fresh tube, the acetone was dried and the remaining supernatant was extracted with 0.75 mL diethyl ether and centrifuged (14 000 g, 1 min, RT), after which the upper organic phase containing free SA was collected. SAG was extracted from the remaining aqueous phase by acidification with 5 µL 1 M HCl and hydrolysis at 80 °C for 1 h, followed by diethyl ether extraction, as described above. All samples were passed through a Supelclean LC-NH₂ SPE column (Supelco, Bellefonte, PA, USA) equilibrated with ether. The column was washed with 1.2 mL chloroform:*n*-propanol (2:1), and samples were eluted with 1.5 mL ether:formic acid (98:2). After drying under a stream of nitrogen, the pellet was resuspended with 0.1 mL dichloromethane:methanol (80:20) and derivatized with 2 µL trimethylsilyl-diazomethane (Sigma-Aldrich, Oakville, Canada) for 20 min at RT. The reaction was terminated by adding 2.1 µL acetic acid in hexane (1:7.5) and incubating

for 30 min at RT. The resulting methyl esters were analysed on a gas chromatograph/mass spectrometer (6890N GC connected to a 5975 mass selective detector; Agilent Technologies, Palo Alto, CA, USA) using a DB-5 capillary column (Agilent Technologies) with flow rate = 1.2 mL min⁻¹ and helium carrier gas. The methyl esters were measured using selected-ion monitoring with *m/z* 153 (SA) and *m/z* 157 ([²H₆]SA).

H₂O₂ determination

H₂O₂ was extracted and measured as previously described (Jiang, Woollard & Wolff 1990) with some modifications. Leaf tissue (0.2 g FW) was flash frozen and ground under liquid N₂ in 1 mL of 0.2 M HClO₄. The homogenate was incubated (5 min, 4 °C) and centrifuged (10 000 g, 10 min, 4 °C), and the supernatant was then removed and neutralized to pH 7–8 with 0.2 M NH₄OH, pH 9.5. After centrifugation (3000 g, 2 min, 4 °C), the supernatant was passed through an AG 1-X8 resin column (Bio-Rad Laboratories, Mississauga, Canada). Following elution from the column with ice-cold distilled water, 0.2 mL of the eluate was combined with 0.5 mL of an assay reagent (0.5 mM (NH₄)₂Fe(SO₄)₂, 50 mM H₂SO₄, 0.2 mM xylenol orange, 200 mM sorbitol). Following incubation (45 min, RT), the absorbance at 560 nm was measured using a spectrophotometer. To evaluate the % recovery of H₂O₂, 5 µmol of H₂O₂ was added directly to the tissue prior to extraction. Recovery ranged from 90 to 95%.

NO determination

NO was assayed using the method described by Murphy & Noack (1994), with some modifications. Leaf tissue (0.15 g FW) was flash frozen and ground under liquid N₂ in 100 mM potassium phosphate buffer (pH 7.0) containing 0.6% (w/v) insoluble PVP. Following addition of powdered activated carbon, the sample was centrifuged (11 000 g, 10 min, 4 °C), and the clarified supernatant was pre-treated for 5 min at RT with 100 U catalase and 50 U SOD (Sigma-Aldrich) to remove ROS. Oxyhaemoglobin was prepared fresh on the day of use by converting 20 mg metHb (Sigma-Aldrich) to Hb using an excess of sodium dithionite (2 mM) in 50 mM Tris pH 7.0. The solution was then oxidized with a stream of O₂ and desalted by passing it through Sephadex G-25 column (GE Healthcare, Mississauga, Canada). Following elution with 50 mM Tris pH 7.0, the concentration of HbO₂ was determined by absorbance at 415 nm (extinction coefficient 131 mM⁻¹ cm⁻¹). HbO₂ (10 µM) was then added directly to the pre-treated samples (see above) and incubated (5 min, RT). The conversion of HbO₂ to metHb was measured by absorbance at 401 and 421 nm. The concentration of NO was calculated as (A₄₀₁HbO₂ - A₄₂₁ metHb) using extinction coefficient of 77 mM⁻¹ cm⁻¹.

Transcript and protein determination

RNA was extracted from leaves and suspension cells using TRIZOL reagent (Invitrogen, Carlsbad, CA, USA)

according to the manufacturer's instructions. Partial cDNAs (to be used as hybridization probes in Northern blot analyses) were amplified from tobacco or *Arabidopsis* leaf RNA using an RT-PCR kit (Access RT-PCR, Promega, Madison, WI, USA) and cloned into pGEM-T Easy plasmid (Promega). Care was taken to generate cDNA probes that minimized complementarity with other known gene family members. The cDNAs were excised from the plasmid and gel purified for use as hybridization probes. The primer sequences used for RT-PCR can be found in Supporting Information Table S1. In the case of tobacco *Aox1a*, a cloned full-length cDNA was used as probe (Vanlerberghe & McIntosh 1996). Northern blot analyses were performed as previously described (Sieger *et al.* 2005). After X-ray film development, blots were quantified by densitometry using ImageJ (National Institutes of Health, USA). Isolation of mitochondria from leaves (starting with 35 g of leaf tissue from 10 plants) and immunoblot analysis of mitochondrial proteins (AOX and *coxII*) were done as previously described (Vanlerberghe *et al.* 1995; Robson & Vanlerberghe 2002).

Tobacco suspension cell experiments

For treatment of suspension cells, a small volume of SA (from a fresh and filter-sterilized 1 M stock solution) was added directly to 200 mL cultures. Culture viability was determined by microscopic observation of a small aliquot of cells treated with 0.025% Evan's Blue, which is excluded from live cells. At least 400 cells were scored to establish the % viability of a culture. For isolation of genomic DNA, tissue (0.2 g FW) was harvested by vacuum filtration, transferred to 1.5 mL screw-cap tubes and flash frozen in liquid N₂. The tissue was homogenized in 0.7 mL extraction buffer [100 mM Tris-HCl, 50 mM ethylenediaminetetraacetic acid (EDTA), 500 mM NaCl, 2% (v/v) sodium dodecyl sulphate, 2% (v/v) β -mercaptoethanol, pH 8.0 containing 1% (w/v) PVP-10 added after autoclaving]. DNA isolation and analysis was then done as previously described (Lin *et al.* 2001; Robson & Vanlerberghe 2002), and also utilizing of general molecular biology protocols (Sambrook & Russell 2001).

SOD activities

All steps were performed at 4 °C. Leaf tissue (0.2 g FW) was flash frozen in liquid N₂ and homogenized in 0.2 mL protein extraction buffer (50 mM KH₂PO₄, 0.2% Triton X-100, 0.05% β -mercaptoethanol, 1% [w/v] PVP-25, pH 7.8). Samples were incubated (10 min, 4 °C) and centrifuged (13 000 g, 10 min, 4 °C), and then aliquots of the supernatant were stored at -80 °C until use. After determination of protein concentration, SOD activity gel staining was performed as previously described (Beauchamp & Fridovich 1971), with some modifications. Non-denaturing gels were pre-equilibrated in a solution containing 0.05 M KH₂PO₄, 1 mM EDTA, pH 7.8, along with the appropriate inhibitors when required (2 mM KCN to inhibit copper zinc SOD [CuZnSOD], 5 mM H₂O₂ to inhibit CuZnSOD and iron

SOD [FeSOD]). After 30 min, the pre-equilibration solution was replaced with a fresh solution containing 0.24 mM nitroblue tetrazolium, 33.2 μ M riboflavin and 0.2% tetramethylethylenediamine. After incubation (30 min, dark, shaking), the gel was illuminated with fluorescent light (400 μ mol m⁻² s⁻¹) for 5 min, or until the gel became uniformly blue except in positions with SOD activity. Individual SOD activities were then analysed using ImageJ.

Imaging of mitochondrial O₂⁻

Imaging of O₂⁻ was performed using the MitoSOX Red mitochondrial O₂⁻ indicator (M36008; Invitrogen) that is selectively accumulated by mitochondria, where it is oxidized by O₂⁻ and becomes fluorescent upon binding to nucleic acid (Robinson, Janes & Beckman 2008). Intact tobacco leaves were inoculated with bacteria as usual. At different times, leaves were removed and the lower epidermis was peeled off. The remaining leaf segments were then floated (30 min, RT, dark) on 3 μ M MitoSOX Red in water. In some cases, leaf was instead loaded (20 min, RT, dark) with 0.35 μ M MitoTracker Red (M7512; Invitrogen), which also selectively accumulates in mitochondria. Samples were then mounted on microscope slides, and the mesophyll cell layer was immediately examined with a LSM510 META laser-scanning confocal microscope (Carl Zeiss, Jena, Germany), with excitation at 488 nm (for MitoSOX Red) or 568 nm (for MitoTracker Red) and detection through a 585–615 nm band-pass filter. Z-series (typically 8–16 μ m in depth with 2 μ m step size) were combined in a maximum intensity projection image using LSM510 imaging software and processed with Adobe Photoshop CS2.

RESULTS

Compatible and incompatible responses of tobacco leaf to *P. syringae* infection

To study the role of the mitochondrion in responses to biotic stress, tobacco leaf was inoculated with three different *P. syringae* pathovars. An initial characterization established that the pathovars resulted in three different interactions. In the case of pv. *tabaci*, this naturally occurring virulent pathogen of tobacco proliferated rapidly over the first two days (Fig. 1a). Measures of leaf conductivity indicated no loss of membrane integrity at 1 d post-inoculation but significant loss of membrane integrity (a measure of cell death) by 2 d (Fig. 1b). Visual observations indicated the appearance of water-soaked tissue and cell death lesions by 2 d, both classic symptoms of the wildfire disease caused by virulent *P. syringae* (Fig. 2). The pv. *maculicola* also proliferated rapidly over the first day (Fig. 1a) but, unlike pv. *tabaci*, this was accompanied by significant cell death as well by 1 d (Fig. 1b) and little further proliferation of the bacteria after 1 d. In this case, the leaf displayed dry lesions (the typical appearance of HR lesions) beginning at 1 d and the tissue was not water-soaked (Fig. 2). In the case of pv. *phaseolicola*, it did not proliferate after inoculation and

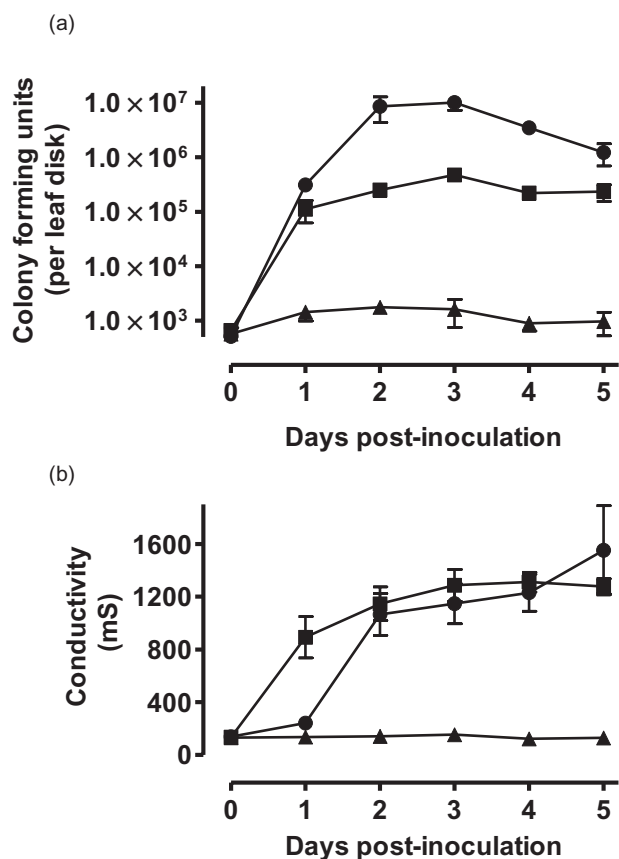


Figure 1. Bacterial proliferation in tobacco leaf (a) and conductivity (ion leakage) of tobacco leaf (b) at different times post-inoculation with pathovars of *Pseudomonas syringae* (closed circle, *tabaci*; closed square, *maculicola*; closed triangle, *phaseolicola*). For bacterial proliferation experiments, bacterial density for inoculation was adjusted to 1×10^5 cfu mL⁻¹. Data are the mean \pm SE of three independent experiments, each of which showed similar results. In some cases, error bars are smaller than the data symbol.

there was no loss of membrane integrity or visual symptoms of cell death or disease (Figs 1 and 2). Summarizing, the results indicate that the interaction of tobacco with *pv. tabaci* is a compatible, disease-causing interaction. The *pv.*

maculicola induces a resistance response (incompatible interaction) that includes an HR-like cell death, which we will refer to hereafter as HR. The *pv. phaseolicola* is an incompatible interaction but without cell death.

Dynamic responses of stress signalling molecules to *P. syringae* infection

To further characterize the plant responses to *P. syringae*, the levels of well-known biotic stress signalling molecules (SA, H₂O₂, NO) were quantitatively measured. In the case of infection with HR-inducing *pv. maculicola*, levels of leaf SA increased rapidly between 3 and 6 h post-inoculation (Fig. 3a). The compatible interaction (*pv. tabaci*) had no effect on SA level at 6 h, although some accumulation of SA was seen by 24 h. In the case of infection with the incompatible (but not HR-inducing) *pv. phaseolicola*, some accumulation of SA occurred by 6 h, but to only 36% of the level seen with *pv. maculicola*. No changes were seen in the level of SAG at 6 h post-inoculation with any of the pathovars, but the level of this biologically inactive form did accumulate to high levels by 24 h in response to both of the incompatible interactions (Fig. 3b). Interestingly, the SA accumulation seen with *pv. maculicola* was clearly biphasic being very high at 6 h, back to lower levels at 12 h and higher again by 24 h.

Just as the two incompatible pathovars had different impacts on leaf SA, they also had distinct impacts on leaf H₂O₂ and NO levels. Changes in H₂O₂ level after inoculation with the HR-inducing *pv. maculicola* were reminiscent of a classic two-phase oxidative burst (with a first and transient peak at 2 h post-inoculation and a second and sustained peak at 8 h), but the variability in this response only allows to conclude that H₂O₂ remained high (Fig. 4a). This was accompanied by a rapid 10-fold accumulation of NO over the first 6 h and further accumulation through 24 h (Fig. 4b). In the case of *pv. phaseolicola*, there was instead a general decline in H₂O₂ level after inoculation. Similarly, there was no rapid accumulation of NO over the first 6 h or high accumulation by 24 h, but rather just a steady and modest accumulation over the full 24 h period.

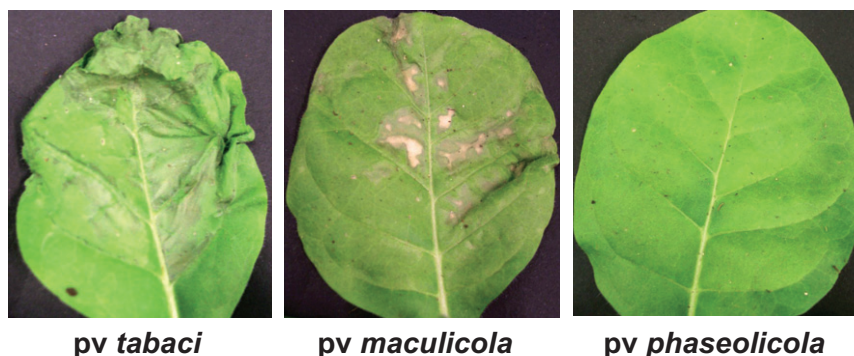


Figure 2. Typical visual symptoms of tobacco leaf at 2 d post-inoculation with pathovars of *Pseudomonas syringae*. See text for details.

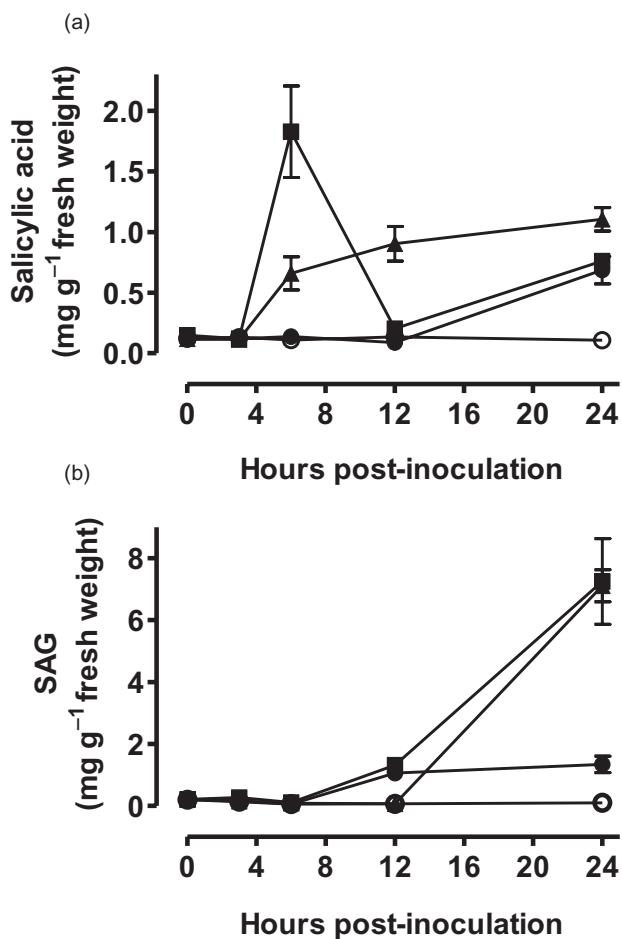


Figure 3. Levels of salicylic acid (a) and salicylic acid β -glucoside (SAG) (b) in tobacco leaf at different times post-mock inoculation with H₂O (open circles) or post-inoculation with pathovars of *Pseudomonas syringae* (closed circle, *tabaci*; closed square, *maculicola*; closed triangle, *phaseolicola*). Data are the mean \pm SE from six separate plants, across two independent experiments. In some cases, error bars are smaller than the data symbol.

Leaf *Aox1a* transcript levels are dynamic but can be studied in response to bacterial inoculations

We found that the transcript level of tobacco *Aox1a* was extremely dynamic over a diurnal cycle, with transcript levels clearly rising during the early part of the light period and then falling during the later part of the light period and through the dark period (Supporting Information Fig. S1A,B). In contrast, transcript encoding phenylalanine ammonia lyase (PAL) peaked during the dark period (Supporting Information Fig. S1C,D). Therefore, to robustly examine *Aox1a* gene expression in response to inoculation with bacteria, it was critical to always perform inoculations at a defined time (5 h into light period) and to normalize all transcript data against control samples (water-infiltrated leaves) taken in parallel with all treatment samples. It was also important to determine that water infiltration alone

was not having a significant effect. To confirm this, *Aox1a* and *PAL* transcript levels were compared in leaves either infiltrated with water or left untreated. Based on these experiments, it was determined that the water infiltration itself was having little, if any, impact (Supporting Information Fig. S1).

Distinct changes in *Aox1a* transcript level and AOX protein level occur in response to different *P. syringae* pathovars

The level of tobacco *Aox1a* transcript was compared up to 48 h after inoculation with different pathovars and also compared with changes in AOX protein level in isolated tobacco leaf mitochondria (Fig. 5, Supporting Information Fig. S2). Three patterns emerged. In the case of *pv. phaseolicola*, there was a strong (but transient) increase in *Aox1a* transcript at 12 h post-inoculation (Fig. 5a, Supporting Information Fig. S2) and this was accompanied by a dramatic increase in AOX protein, as measured at 24 h

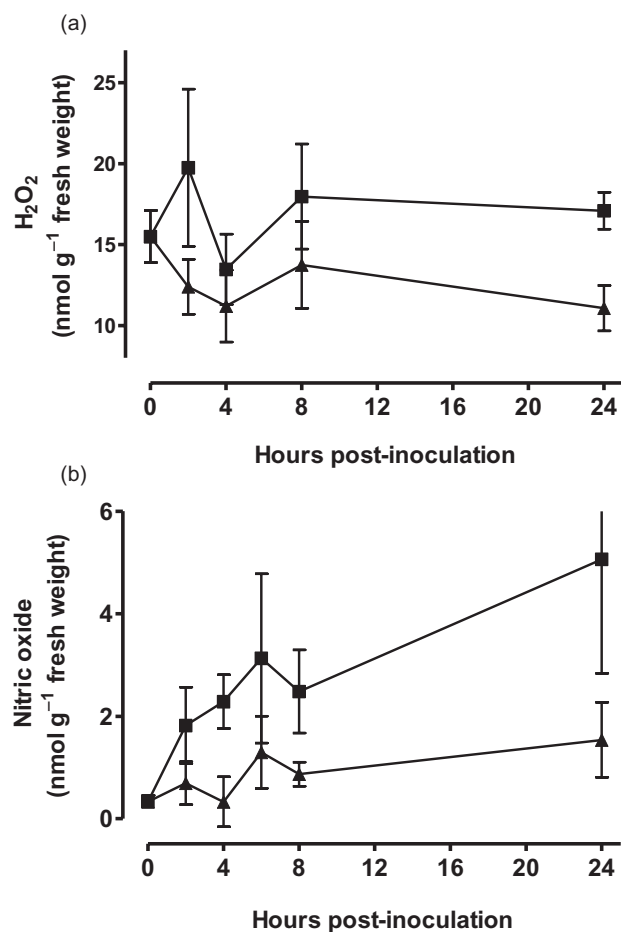


Figure 4. Levels of H₂O₂ (a) and NO (b) in tobacco leaf at different times post-inoculation with pathovars of *Pseudomonas syringae* (closed square, *maculicola*; closed triangle, *phaseolicola*). Data are the mean \pm SE of four independent experiments, each of which showed similar results.

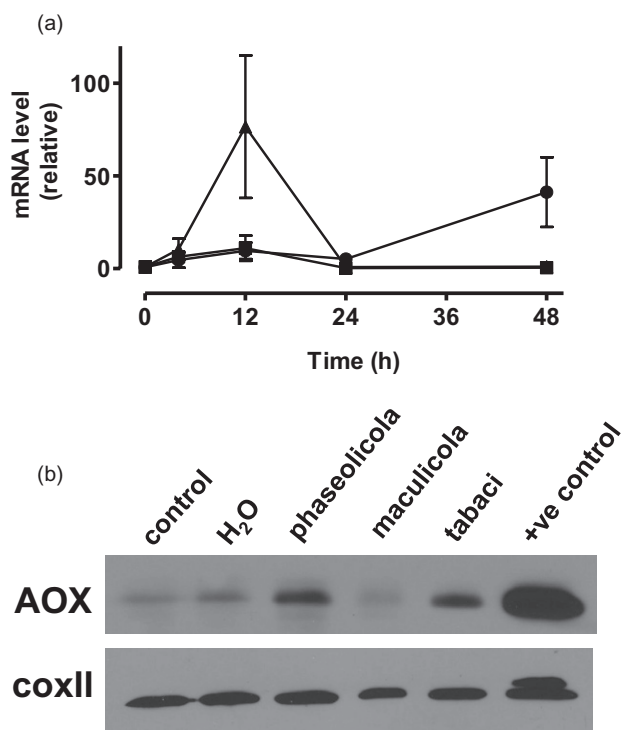


Figure 5. Level of *Aox1a* transcript (a) and alternative oxidase (AOX) protein (b) in tobacco leaf at different times post-inoculation with pathovars of *Pseudomonas syringae* (closed circle, *tabaci*; closed square, *maculicola*; closed triangle, *phaseolicola*). Data in (a) is the mean \pm SE of densitometer analysis of Northern blots from three independent experiments normalized for diurnal changes in *Aox1a* transcript level, each of which showed similar results. For these data, the level of mRNA at each time point in mock-inoculated plants was arbitrarily set to 1 and used to normalize the data for plants inoculated with bacteria. Quality of RNA and confirmation of equal loading between lanes was routinely checked by ethidium bromide staining (not shown). For (b), mitochondria were isolated from tobacco leaf at 24 h after treatments. The mitochondrial proteins (100 μ g) were then separated by SDS-PAGE, transferred to nitrocellulose and probed with an antibody against AOX. Confirmation of sample quality and equal loading between lanes was routinely checked by also examining levels of cytochrome oxidase subunit II (coxII) protein in the isolated mitochondria, as shown. The lane labelled H₂O are leaves infiltrated with H₂O while the lane labelled +ve control is a mitochondrial sample isolated from a transgenic tobacco line overexpressing AOX. Representative results are shown.

(Fig. 5b). However, in the case of the HR-inducing pv. *maculicola*, there was little if any change in *Aox1a* mRNA or protein in comparison to water-infiltrated controls. Similarly, pv. *tabaci* did not result in an early accumulation of *Aox1a* transcript, although a late accumulation at 48 h, when disease symptoms and necrotic cell death were already prevalent, was clearly evident. In this case, some increase in AOX protein was also already evident at 24 h.

For comparison, we examined AOX expression in *Arabidopsis* responding to *P. syringae* pv. *tomato*. In this case, both DC3000 (a virulent strain that caused necrotic cell death by 48 h) and DC3000 (*avrRpt2*) (an incompatible

strain that induced the HR by 24 h) caused similar and modest induction of *Aox1a*, particularly at later stages (12–48 h) (Supporting Information Fig. S3). These results are generally similar to those found in a previous study (Simons *et al.* 1999). In the case of DC3000 (*avrRps4*) (an incompatible strain that did not induce HR), there was little change in *Aox1a* expression in comparison to control. We also examined the expression of other *Arabidopsis* AOX genes. A change in transcript level of *Aox1d* in response to each bacterial strain was similar to that seen with *Aox1a*, although the overall level of transcript was much less (data not shown). Levels of *Aox1c* and *Aox2* were not impacted by the treatments (data not shown).

Other biotic stress-related genes are also differentially expressed in response to different *P. syringae* pathovars

Changes in tobacco *Aox1a* transcript were compared with that of other tobacco genes previously shown to respond to biotic stress. *HSR203J* and *HINI* have each been previously judged as good marker genes for the HR response (Pontier *et al.* 1994; Gopalan, Wei & He 1996). Similarly, increased *PAL* gene expression is often associated with the HR (Vlot *et al.* 2009). These genes were all strongly induced within 4 h of inoculation with pv. *maculicola* (Fig. 6a–c). In the case of *HSR203J* and *HINI*, there was also a later (12 h) induction by pv. *phaseolicola*. All three genes were only induced by pv. *tabaci* at a much later stage (24–48 h). *PR-1* is a well-known late-induced, SA-responsive defence gene to incompatible pathogens (Eulgem 2005). As expected, *PR-1* transcript did not change significantly until 24 h, at which time it was induced by the incompatible interactions (strongly by pv. *phaseolicola* and more moderately by pv. *maculicola*) (Fig. 6e). The compatible pv. *tabaci* did not induce *PR-1* through 48 h. *GRAS* likely encodes a transcription factor and its transcript level has previously been shown to respond to treatments such as antimycin A, NO, SA and H₂O₂, in a manner very similar to that of *Aox1a* (Maxwell, Nickels & McIntosh 2002). *GRAS* transcript was transiently induced (at 12 h) by pv. *phaseolicola*, not induced at all by pv. *maculicola*, and induced only late by pv. *tabaci* (Fig. 6f). These patterns mirror that seen with *Aox1a* transcript (Fig. 5a). Increased ethylene production is a common response to biotic stress (van Loon, Geraats & Linthorst 2006). The gene encoding ACC oxidase, which catalyses the last step in ethylene biosynthesis, increased transiently (at 12 h) in response to all these pathovars but most strikingly in response to pv. *maculicola* (Fig. 6d).

Qualitatively similar changes in *Aox1a* transcript abundance can be seen in tobacco suspension cells treated with different concentrations of SA

Treatment of tobacco suspension cells with different concentrations of SA led to differences in the timing, extent

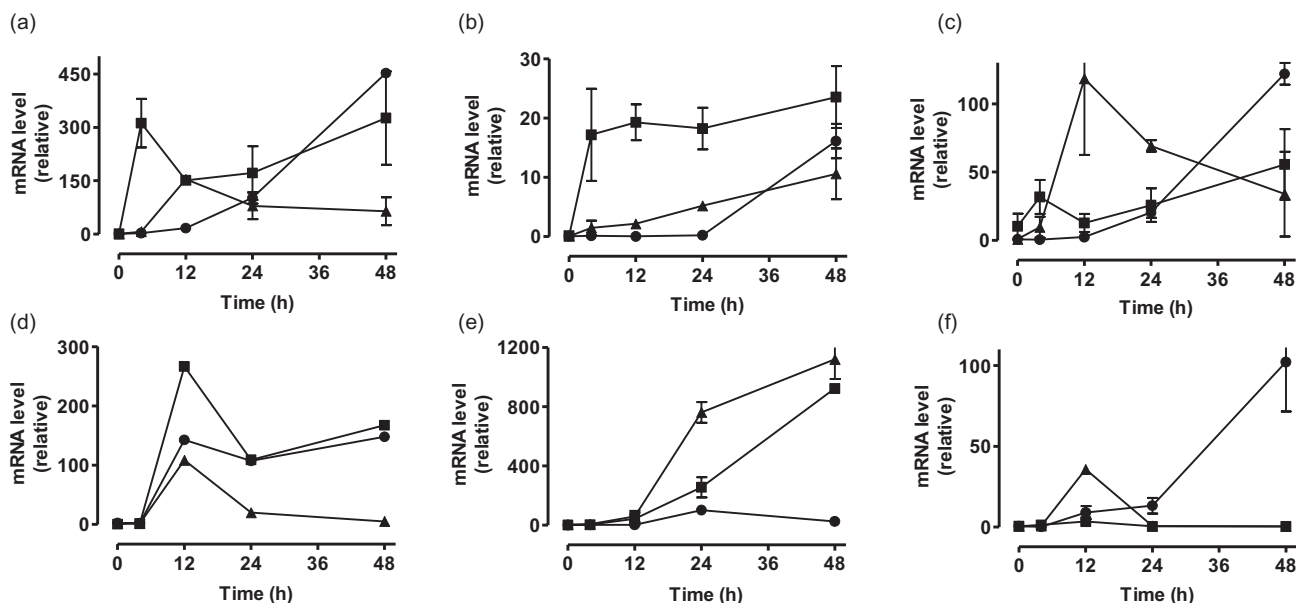


Figure 6. Level of *HSR203J* (a), *PAL* (b), *HINI* (c), *ACC oxidase* (d), *PR-1* (e) and *GRAS* (f) transcript in tobacco leaf at different times post-inoculation with pathovars of *Pseudomonas syringae* (closed circle, *tabaci*; closed square, *maculicola*; closed triangle, *phaseolicola*). Data are the mean \pm SE of densitometer analysis of Northern blots from two independent experiments, each of which showed similar results. For these data, the level of mRNA in the mock-inoculated plants has been arbitrarily set to 1 and used to normalize the data for plants inoculated with bacteria. Quality of RNA and confirmation of equal loading between lanes was routinely checked by ethidium bromide staining (not shown).

and type of cell death by the culture. It was therefore of interest to see what change in *Aox1a* gene expression accompanied these responses and whether these mirrored the changes seen during the response of tobacco leaf to the different bacterial pathovars.

A high concentration of SA (3 mM) led to rapid cell death, with complete death of the culture within 24 h (Fig. 7a). This was accompanied by a distinct pattern of breakdown of high-molecular-weight DNA to generate the low-molecular-weight 'DNA ladder' typical of PCD. As expected, this 'ladder' has bands of DNA corresponding in size to that of oligonucleosomal fragments (~180–200 bp) and multiples thereof (Fig. 7b). In contrast, treatment with a moderate concentration of SA (0.5 mM) led to a slower death of the culture, with only ~30% of cells dead by 24 h and ~85% by 48 h. This cell death was also accompanied by the breakdown of high-molecular-weight DNA but did not generate the DNA ladder typical of PCD, indicating that in this case, the death was necrotic. Low (0.1 mM) SA had little impact on cell viability (Fig. 7a) and cultures maintained high-molecular-weight DNA through 120 h (Fig. 7b).

The SA treatments led to distinct changes in *Aox1a* gene expression. With the treatment that did not induce significant cell death (0.1 mM SA), there was a rapid (within 2 h), large and transient induction of *Aox1a* transcript (Fig. 7c,d). With the treatment generating PCD (3.0 mM SA), there was no induction, but rather a slight decline in *Aox1a* transcript. With the treatment causing necrotic cell death (0.5 mM), there was also no early induction by 2 h but rather an induction in the longer term.

SOD enzymes show distinct changes in activity in response to different *P. syringae* pathovars

The major SOD enzymes (MnSOD, CuZnSOD, FeSOD) were identified on activity gels according to their sensitivity to different inhibitors. The gels were then used to monitor the activity of each enzyme over a 48 h period following inoculation of tobacco leaf. All three enzymes, but particularly CuZnSOD, increased in activity by 24 h, and further by 48 h, following inoculation with *pv. phaseolicola* (Fig. 8). In the case of *pv. tabaci*, none of the activities changed by 24 h. A small increase in MnSOD and CuZnSOD activity did appear, however, by 48 h, with still no change in FeSOD. In response to *pv. maculicola*, the activity of CuZnSOD and FeSOD perhaps increased over the 48 h period, while MnSOD clearly declined by 24 h and further by 48 h. In summary, the activities of all three enzymes tended to increase or remain unchanged in response to all three pathovars, with the exception of MnSOD activity following inoculation with the HR-inducing *pv. maculicola*, in which case, activity declined dramatically (Fig. 8).

Dynamic changes in mitochondrial O_2^- level in response to different *P. syringae* pathovars

Mitochondrial O_2^- level in tobacco leaf mesophyll cells was assessed by using confocal microscopy to image MitoSOX Red fluorescence. To ensure no confounding effects due to autofluorescence, images of unlabelled tissue were obtained using the acquisition settings and longest exposure time

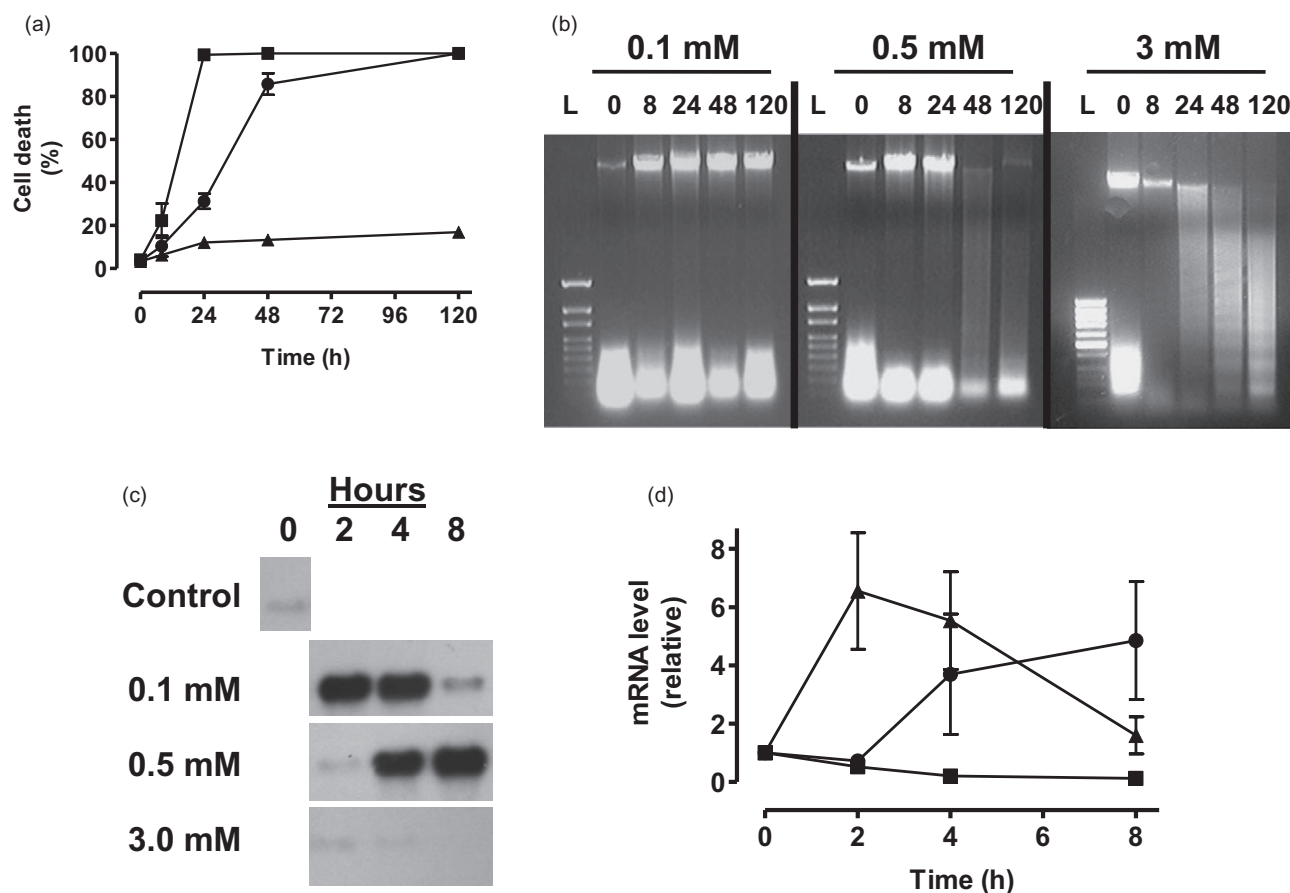


Figure 7. Effects of SA on tobacco suspension cells. (a) Viability of suspension cell cultures following treatment with 0.1 mM (triangle), 0.5 mM (circle) or 3 mM (square) salicylic acid (SA). Data are the mean \pm SE of two independent experiments. Note that in some cases, error bars are smaller than the data symbol. (b) Representative agarose gel analysis of DNA extracted from suspension cells at different times after treatment with 0.1, 0.5 or 3.0 mM SA. The lane marked L is a 100 bp low-molecular-weight DNA ladder, but please note that the commercial ladder corresponding with the 3 mM lanes differs from that corresponding with the 0.1 and 0.5 mM lanes. The estimated size of the low-molecular-weight bands of DNA seen to accumulate in the 3 mM (48 h) and 3 mM (120 h) lanes are ~170, 350, 550 and 770 bp. (c) Representative Northern blot showing changes in the level of *Aox1a* transcript in suspension cells at different times after treatment with 0.1, 0.5 or 3.0 mM SA. (d) Level of *Aox1a* transcript in suspension cells at different times after treatment with 0.1 mM (triangle), 0.5 mM (circle) or 3.0 mM (square) SA. Data are the mean \pm SE of densitometer analysis of Northern blots from three independent experiments, each of which showed similar results. Note that the level of *Aox1a* in control (untreated) cells (time 0 h) was arbitrarily set at 1.

being used for labelled samples. Chlorophyll autofluorescence was detected through a 650 nm long-pass filter, but no signal was detected in the 585–615 nm range. As another control, leaf segments with the lower epidermis removed were floated on solution containing the Complex III inhibitor antimycin A (10 μ M, 1 h, RT) prior to loading with MitoSOX Red and, as expected, this dramatically elevated MitoSOX Red fluorescence. There are reports that MitoSOX Red can cause mitochondrial rupture and signal relocation to the nucleus at higher concentration (Robinson *et al.* 2008) and we did observe labelling of nuclei. However, we observed no visible difference in the number of mitochondria in leaf labelled with MitoSOX Red compared to Mitotracker Red (data not shown).

In leaves inoculated with the HR-inducing *pv. maculicola*, high levels of O_2^- were clearly evident by 4 h post-inoculation, the earliest time point examined, and persisted

through 24 h (Fig. 9). In contrast, there was little change in O_2^- level, compared to mock-inoculated leaves, at any time point following inoculation with *pv. phaseolicola*. Finally, *pv. tabaci* induced only a late (24 h) increase in O_2^- but not the early mitochondrial O_2^- burst seen in response to *pv. maculicola* (Fig. 9).

DISCUSSION

Research suggests that the mitochondrion can be an important intracellular source of ROS during plant PCD, generating a so-called mitochondrial oxidative burst. Since AOX is an important regulator of ROS generation by the ETC, several studies have examined the relationship between AOX and susceptibility to PCD induced by various biotic or abiotic stimuli. For example, overexpression of AOX in transgenic *Arabidopsis* protoplasts was found to protect

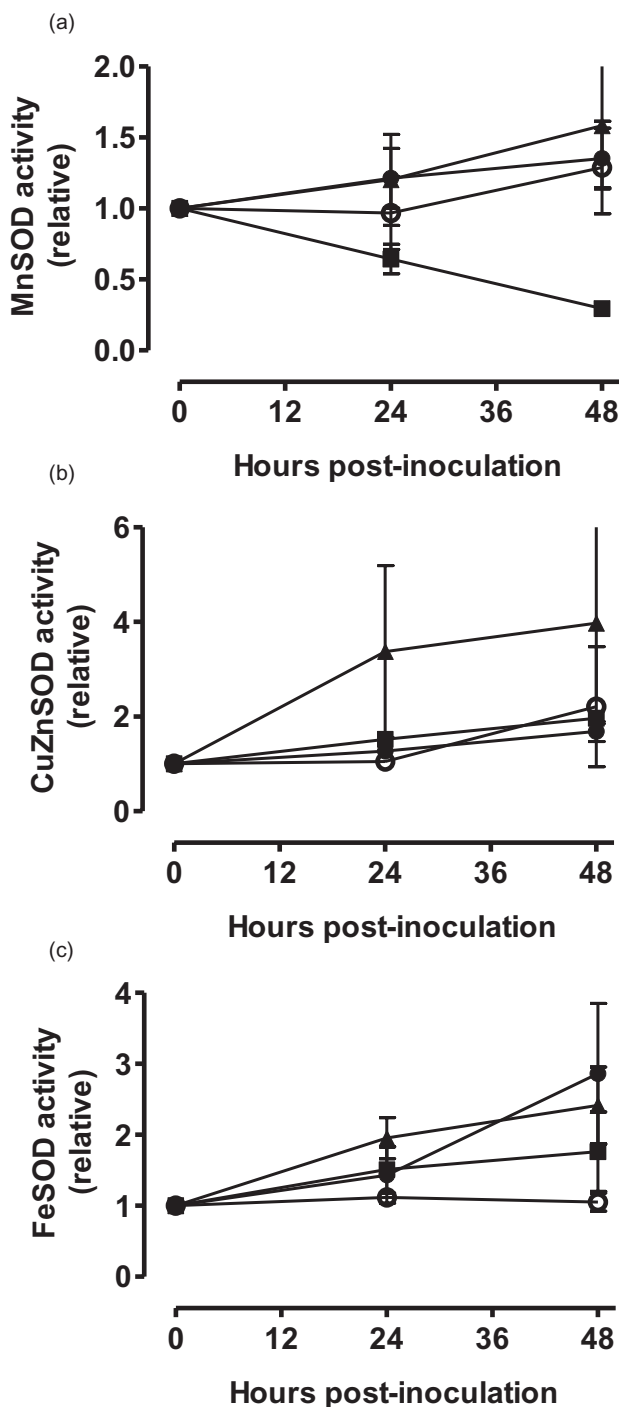


Figure 8. Superoxide dismutase activity in tobacco leaf at different times post-mock inoculation with H₂O (open circle) or post-inoculation with pathovars of *Pseudomonas syringae* (closed circle, *tabaci*; closed square, *maculicola*; closed triangle, *phaseolicola*). An in-gel activity assay was used to separate the activity of MnSOD (a), CuZnSOD (b) and FeSOD (c). Data are the mean \pm SE of three independent experiments, each of which showed similar results. Note that in some cases, error bars are smaller than the data symbol.

against aluminium-induced PCD (Li & Xing 2011), while overexpression in tobacco resulted in slightly smaller tobacco mosaic virus-induced HR lesions (Ordog, Higgins & Vanlerberghe 2002). Conversely, suppression of AOX in transgenic tobacco suspension cells increased their susceptibility to SA or H₂O₂-induced PCD (Robson & Vanlerberghe 2002; Amirsadeghi *et al.* 2006). Collectively, such studies suggest that AOX may provide a level of protection against PCD. Given this, we postulated that during natural examples of PCD that are likely of benefit to the plant (such as the HR), AOX (with its potential to act as a negative regulator of PCD) would not be induced, or might even decline, such as to promote the response. To test this, we compared responses to three different *P. syringae* pathovars. The differential responses to these pathovars was first characterized by examining the kinetics of cell death, changes in key biotic stress signalling molecules and changes in established biotic stress-related genes. These analyses established three distinct plant responses to the pathovars: a compatible response that did not elicit typical defences, such as increased SA, and which was associated, at a late stage, with disease-associated necrotic cell death (*pv. tabaci*); an incompatible response that included well-known defence responses, such as increased SA and *PR-1* transcript, but did not include any HR cell death (*pv. phaseolicola*); and an incompatible response that included strong defence responses (such as rapid accumulation of SA, NO and H₂O₂, and induction of HR-associated genes) and the HR, which was then able to restrict any further proliferation of the pathogen (*pv. maculicola*).

During an HR-inducing interaction, AOX expression is not elevated despite a strong increase of potentially inductive signalling molecules

The signalling molecules SA, NO and H₂O₂ have each been shown to strongly induce AOX in numerous species and contexts, and these molecules all showed an early and strong accumulation in response to the HR-inducing *pv. maculicola*. In addition, the strong induction of ACC oxidase gene expression is an indirect evidence that ethylene was likely also being produced, as has previously been documented in the HR response of tobacco to *P. syringae* (Mur *et al.* 2008). Ethylene is strongly implicated in the induction of AOX by abiotic stress (Ederli *et al.* 2006). However, despite the increase of these signalling molecules, there was no increase in *Aox1a* transcript or AOX protein in response to *pv. maculicola*. Hence, during the HR, AOX expression was uncoupled from several of the signalling molecules thought to otherwise promote its induction. In contrast, *pv. phaseolicola* (which induced defence responses, but in the absence of a HR) did elicit a strong transient increase in *Aox1a* transcript, accompanied by increased AOX protein. In the case of *pv. tabaci*, AOX expression was induced but only much later after infection, just prior to necrotic death of the diseased tissue.

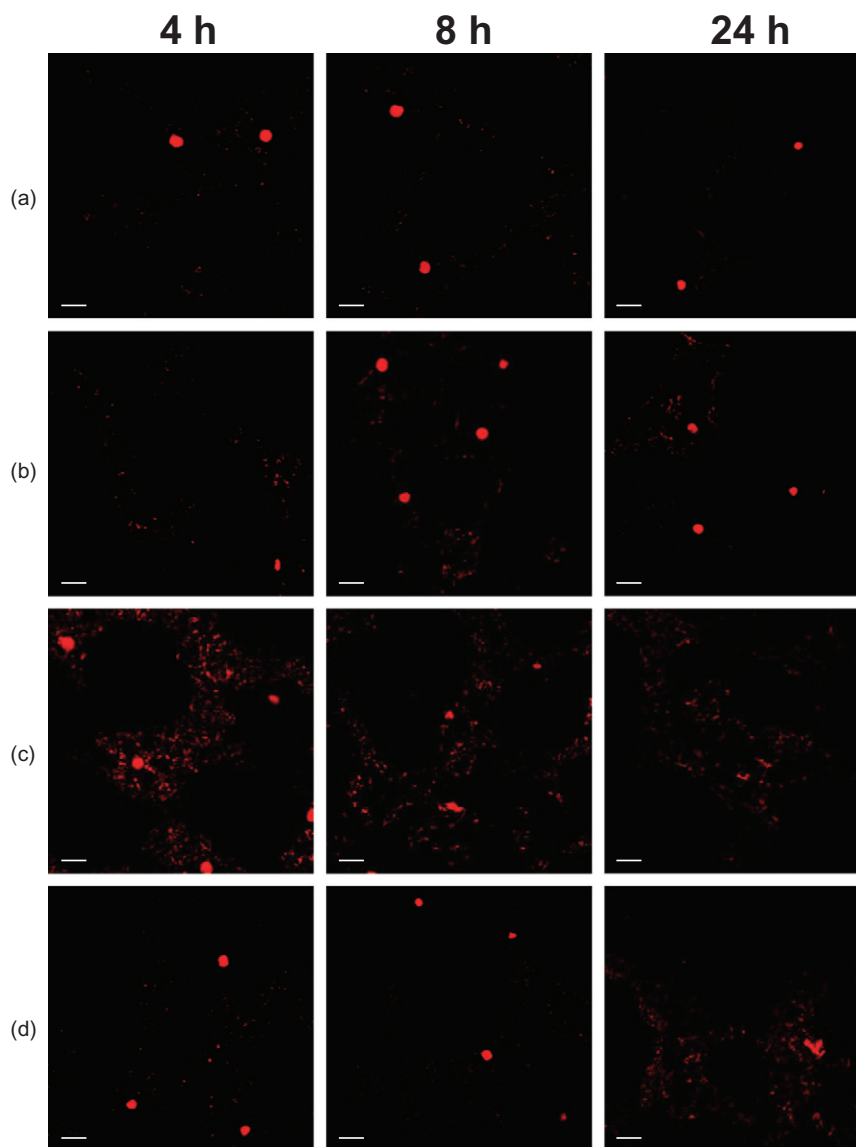


Figure 9. Laser-scanning confocal microscope images of mitochondrial O_2^- in mesophyll cells at different times post-mock inoculation with H_2O (a) or post-inoculation with pathovars of *Pseudomonas syringae*: pv. *phaseolicola* (b), pv. *maculicola* (c) and pv. *tabaci* (d). All images are maximum intensity projections of Z-series (8–16 μm in depth) and are representative results from four independent experiments, each of which showed similar results. Scale bar = 20 μm .

Our results with tobacco differ from a previous study in *Arabidopsis* (Simons *et al.* 1999). It showed that both a compatible and an HR-inducing incompatible *P. syringae* induced *Aox1a*, but with the earliest and strongest induction occurring during the HR. In that study, *Aox1a* was induced strongly by 6 and 22 h after infection with incompatible bacteria, and the authors state that HR tissue collapse occurred by 24 h, although the cell death was not characterized any further. We also observed an increase in *Arabidopsis Aox1a* transcript by both compatible strain DC3000 and HR-inducing strain DC3000 (*avrRpt2*). Furthermore, *Aox1a* was not induced during the incompatible response to DC3000 (*avrRps4*) that lacked the HR.

However, the absolute changes in *Aox1a* transcript that we observed in *Arabidopsis* were much more subtle than we would see, for example, in tobacco responding to pv. *phaseolicola*. Lacomme & Roby (1999) also identified *Aox1a* as a gene induced in *Arabidopsis* suspension cells by an avirulent, but not virulent, *Xanthomonas campestris* and suggested it as an early marker of the HR. However, it is unclear from that study whether the treatment of suspension cells with the avirulent bacteria was actually inducing cell death. Studies in citrus and lettuce leaf have also noted AOX induction in response to HR-inducing bacteria (Kiba *et al.* 2008; Daurelio *et al.* 2009), while harpin, an HR-inducing bacterial elicitor, increased *Aox1a* expression

in *Arabidopsis* suspension cells (Krause & Durner 2004) and AOX activity in *Nicotiana sylvestris* (Vidal *et al.* 2007). Similar to our findings, a few other reports have suggested that AOX is in fact not induced during a PCD response. In tobacco cells challenged by metabolic products of a fungal pathogen that induced PCD, it was noted that AOX capacity was reduced (Cheng *et al.* 2011). However, total respiration was also strongly reduced and AOX transcript and protein were not examined, hence making a complete interpretation of those results difficult. Similarly, AOX was not induced by harpin in *N. sylvestris* leaf (Boccaro *et al.* 2001). Overall, the contrasting results suggest that there may be fundamental differences between species regarding the role of AOX in cell death programs, factors regulating AOX gene expression or baseline AOX level between species. Some differences between studies may also be due to differences in experimentation and interpretation. Our study had the advantage of being able to directly compare multiple distinct responses to different bacterial pathogens, accompanied by direct measures of cell death, changes in signalling molecules (SA, NO, H₂O₂), changes in mitochondrial O₂⁻ and careful characterization of *Aox1a* against background diurnal changes in expression, diurnal changes that have also been previously reported in tobacco (Duttilleul *et al.* 2003). In addition, our studies have been done *in planta* (rather than suspension cells where oxidative poise may differ; Halliwell 2003), and in response to bacteria rather than an HR-inducing elicitor, that might not 'elicit' the same or complete plant response as that of live bacteria (Mur, Kenton & Draper 2005).

At present, we do not know the mechanism by which *Aox1a* expression is suppressed during the HR, despite the dramatically increased level of potential inductive signalling molecules. A clue to this might be provided by the experiment on suspension cells in which it was clear that while low concentrations of SA were highly effective at inducing *Aox1a*, higher concentrations of SA had no effect. This suggests that either high concentrations of SA itself or some downstream consequence of high SA triggers a suppression rather than induction of *Aox1a* expression. Significantly, the cell results mirror well the relationship between *Aox1a* expression, SA level and cell fate seen in leaf during the incompatible interactions. The HR-inducing pv. *maculicola* showed the strongest early induction of SA, lacked any *Aox1a* induction and resulted in PCD. Alternatively, pv. *phaseolicola* showed less early accumulation of SA, a strong transient *Aox1a* induction and no PCD.

Similar to our results, several studies have noted that AOX expression can be strongly induced at the late stages of compatible bacterial interactions that culminate in a disease-associated cell death, or other cases of necrotic cell death. Examples are reported in *Arabidopsis* (Simons *et al.* 1999), lettuce (Kiba *et al.* 2009) and wheat (Sugie, Murai & Takumi 2007). The late AOX induction may represent an extreme response to a collapse of energy metabolism or a non-specific response to cellular dysfunction.

Do AOX and MnSOD act in a coordinated manner to define the strength and specificity of a ROS signal from the mitochondrion?

Our results indicate that MnSOD activity declines in tobacco leaf in response to the HR-inducing pv. *maculicola*. This was distinct from the response of MnSOD activity to the other pathogens, as well as from the response of the other SOD enzymes, which tended to either increase or remain unchanged. Particularly, the increase in CuZnSOD is consistent with previous studies (Kliebenstein *et al.* 1999). However, to our knowledge, few studies have examined changes in MnSOD activity during PCD or in response to biotic stress. A microarray analysis of senescence in *Arabidopsis* suspension cells did report a decrease in both AOX and MnSOD transcript, although heat shock-induced PCD had the opposite effect on both genes (Swidzinski, Sweetlove & Leaver 2002). Also interesting in this respect is a *N. sylvestris* cytoplasmic male-sterile mutant (CMSII) that exhibits both a higher constitutive level of AOX and MnSOD, and a delayed senescence phenotype (Duttilleul *et al.* 2003). It was also shown that PCD of barley aleurone cells is preceded by a loss of SOD activity, with MnSOD appearing to be the first to decline (Fath, Bethke & Jones 2001).

At present, we do not know the mechanism responsible for loss of MnSOD activity in response to pv. *maculicola*. A previous study showed that loss of MnSOD activity during fruit senescence correlated with carbonylation of the protein (Qin *et al.* 2009). Interestingly, human MnSOD is inactivated by ONOO⁻ via tyrosine nitration (Castro *et al.* 2011). Recently, ONOO⁻, which is formed by reaction of NO with O₂⁻, has been shown to accumulate during the HR (Gaupels *et al.* 2011).

There are also means by which the low constitutive level of AOX protein that still exists in tobacco leaf after pv. *maculicola* infection could be inactivated. For example, a high level of H₂O₂ has the potential to convert AOX to its oxidized low activity form (Vanlerberghe, Yip & Parsons 1999). AOX activity is also sensitive to the lipid peroxidation product 4-hydroxy-2-nonenal (Winger, Millar & Day 2005) and, interestingly, was identified as a target of tyrosine nitration in sunflower hypocotyls (Chaki *et al.* 2009).

A major finding of our study is that the HR of tobacco leaf is preceded by an early and persistent mitochondrial burst of O₂⁻. Studies have shown that ROS are important signalling molecules, and that the type of ROS (e.g., O₂⁻ versus H₂O₂), the level of ROS and the location of the ROS will impact the cellular programs that they elicit (Apel & Hirt 2004; Foyer & Noctor 2005; Mittler *et al.* 2011). We suggest that AOX and MnSOD are uniquely positioned to impact both the strength and specificity of ROS signals in the mitochondrion (Fig. 10). AOX will impact the *strength* of the ROS signal by modulating the rate of O₂⁻ generation by the ETC. Then, the activity of MnSOD (the sole enzymatic means to scavenge matrix O₂⁻ and convert it to H₂O₂) will determine the *specificity* of the signal by determining the relative levels of O₂⁻ and H₂O₂ in the matrix. In

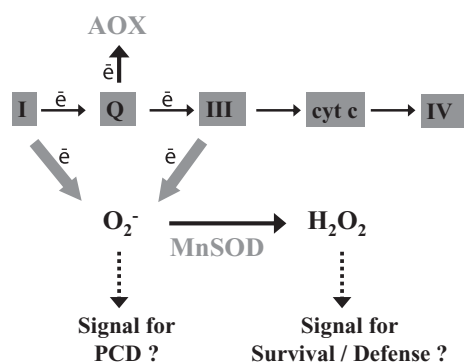


Figure 10. Reactive oxygen species (ROS) are important signalling molecules and the type of ROS (e.g., O_2^- versus H_2O_2), level of ROS and location of ROS impact the cellular programs that they elicit. The model outlined here suggests that alternative oxidase (AOX) and MnSOD are uniquely positioned to impact both the strength and specificity of ROS signals in the mitochondrion. AOX will impact the *strength* of the ROS signal by modulating the rate of O_2^- generation by the mitochondrial ETC. Then, the activity of MnSOD (the sole enzymatic means to scavenge matrix O_2^- and convert it H_2O_2) will determine the *specificity* of the signal by determining the relative levels of O_2^- and H_2O_2 in the matrix. Since H_2O_2 is membrane-permeable, while O_2^- is not, MnSOD may also influence the distribution of mitochondrial-generated ROS between mitochondrion and cytosol. We propose that the suppression of both AOX and MnSOD seen in this study during the HR of tobacco to *Pseudomonas syringae* pv. *maculicola* is important to generating the early and persistent mitochondrial O_2^- burst that was observed. More generally, a coordinated activity of AOX and MnSOD represents a potential means to construct multiple distinct mitochondrial ROS signatures that could lead to distinct cellular responses.

addition, since H_2O_2 is membrane permeable, while O_2^- is not, MnSOD may also influence the distribution of mitochondrial-generated ROS between the mitochondrion and the cytosol (Fig. 10).

Numerous studies have shown a suppression of different ROS-scavenging systems during the HR and other forms of PCD, and it has been suggested that this aspect of the cellular response is necessary to allow a sufficient accumulation of ROS needed to promote the PCD (Foyer & Noctor 2005; Vlot *et al.* 2009). Most studies to date have examined suppression of the ROS-scavenging systems of the cytosol, chloroplast and peroxisome, relating this then to ROS sources such as NADPH oxidase, photosynthesis and photorespiration. Consistent with the theme, we suggest that coordinated suppression of AOX and MnSOD is important in defining a mitochondrial O_2^- burst during the HR.

Is mitochondrial O_2^- an important signal for the HR?

Our results show that mitochondrial O_2^- increases dramatically during the response of tobacco to the HR-inducing pv. *maculicola* and suggest that this response is the result of a coordinated suppression of AOX and MnSOD. This leads to

the important question of whether mitochondrial O_2^- is in fact an important signal for the HR. While it is generally accepted that H_2O_2 , O_2^- , NO and likely other reactive nitrogen species are important players in the initiation and execution of the HR and other defence responses, the detail of their roles requires further investigation. The *Arabidopsis* spontaneous cell death mutant *lsd1* has highlighted the specific importance of O_2^- , particularly when in combination with SA, to promote PCD (Mazel & Levine 2001; Epple *et al.* 2003). Unlike wild-type, *lsd1* does not induce CuZnSOD in response to SA, and the increased O_2^- increases their susceptibility to SA-induced PCD.

One hypothetical means by which mitochondrial O_2^- might be acting mechanistically to promote PCD is via its reaction with NO to produce ONOO⁻. ONOO⁻ could impact the function of proteins via the nitration of key tyrosine residues and studies have just begun to identify those proteins subject to tyrosine nitration during the HR (Ceccconi *et al.* 2009). Alternatively, some of the pro-survival functions described for NO (Yun *et al.* 2011) might be attenuated if NO is being scavenged by O_2^- . Similarly, some of the pro-survival functions described for H_2O_2 (Torres, Jones & Dangl 2006) might be attenuated in the absence of conversion of mitochondrial O_2^- to H_2O_2 . We previously suggested that complex III-derived O_2^- could induce PCD in tobacco suspension cells, based on the disparate susceptibility of cells to two complex III inhibitors with differential capacities to generate O_2^- (Robson, Zhao & Vanlerberghe 2008). Elucidating the functional importance of the mitochondrial O_2^- burst clearly represents a rich area for further study.

While we have emphasized the importance of a mitochondrial O_2^- burst as a potential pro-death signal in support of the HR, it is worth noting that the strong induction of AOX, and to a lesser extent MnSOD, during the response to pv. *phaseolicola* might also be of importance. In this case, the lower overall mitochondrial-generated ROS, along with perhaps a shift toward H_2O_2 , at the expense of O_2^- , might be an important pro-survival signal to prevent HR and/or induce other defence gene expression. Hence, we view the coordinated activity of AOX and MnSOD as a potential means to construct multiple distinct mitochondrial ROS signatures that could lead to distinct cellular responses (Fig. 10).

ACKNOWLEDGMENTS

The authors thank Dr K. Yoshioka, Dr W. Moeder and Dr R. Harrison, each at University of Toronto, for the different bacteria, assistance with SA analysis and advice on fluorescence imaging, respectively. We gratefully acknowledge the financial support of the Natural Sciences and Engineering Research Council of Canada.

REFERENCES

Amirsadeghi S., Robson C.A., McDonald A.E. & Vanlerberghe G.C. (2006) Changes in plant mitochondrial electron transport

- alter cellular levels of reactive oxygen species and susceptibility to cell death signaling molecules. *Plant and Cell Physiology* **47**, 1509–1519.
- Amirsadeghi S., Robson C.A. & Vanlerberghe G.C. (2007) The role of the mitochondrion in plant responses to biotic stress. *Physiologia Plantarum* **129**, 253–266.
- Apel K. & Hirt H. (2004) Reactive oxygen species: metabolism, oxidative stress, and signal transduction. *Annual Review of Plant Biology* **55**, 373–399.
- Arpagaus S., Rawlyer A. & Braendle R. (2002) Occurrence and characteristics of the mitochondrial permeability transition in plants. *Journal of Biological Chemistry* **277**, 1780–1787.
- Ashtamker C., Kiss V., Sagi M., Davydov O. & Fluhr R. (2007) Diverse subcellular locations of cryptogein-induced reactive oxygen species production in tobacco Bright Yellow-2 cells. *Plant Physiology* **143**, 1817–1826.
- Beauchamp C. & Fridovich I. (1971) Superoxide dismutase: improved assays and an assay applicable to acrylamide gels. *Analytical Biochemistry* **44**, 276–287.
- Boccarda M., Boué C., Garmier M., De Paepe R. & Boccarda A.-C. (2001) Infra-red thermography revealed a role for mitochondria in pre-symptomatic cooling during harpin-induced hypersensitive response. *The Plant Journal* **28**, 663–670.
- Braidot E., Petrusa E., Vianello A. & Macri F. (1999) Hydrogen peroxide generation by higher plant mitochondria oxidizing complex I or complex II substrates. *FEBS Letters* **451**, 347–350.
- Castro L., Demicheli V., Tórtora V. & Radi R. (2011) Mitochondrial protein tyrosine nitration. *Free Radical Research* **45**, 37–52.
- Cecconi D., Orzetti S., Vandelle E., Rinalducci S., Zolla L. & Delledonne M. (2009) Protein nitration during defense response in *Arabidopsis thaliana*. *Electrophoresis* **30**, 2460–2468.
- Chaki M., Valderrama R., Fernández-Ocaña A.M., et al. (2009) Protein targets of tyrosine nitration in sunflower (*Helianthus annuus* L.) hypocotyls. *Journal of Experimental Botany* **60**, 4221–4234.
- Cheng D.-D., Jia Y.-J., Gao H.-Y., Zhang L.-T., Zhang Z.-S., Xue Z.-C. & Meng Q.-W. (2011) Characterization of the programmed cell death induced by metabolic products of *Alternaria alternata* in tobacco BY-2 cells. *Physiologia Plantarum* **141**, 117–129.
- Coll N.S., Eppie P. & Dangl J.L. (2011) Programmed cell death in the plant immune response. *Cell Death and Differentiation* **18**, 1247–1256.
- Daurelio L.D., Checa K., Barrio J.M., Ottado J. & Orellano E.G. (2009) Characterization of *Citrus sinensis* type 1 mitochondrial alternative oxidase and expression analysis in biotic stress. *Bio-science Reports* **30**, 59–71.
- van Doorn W.G., Beers E.P., Dangl J.L., et al. (2011) Morphological classification of plant cell deaths. *Cell Death and Differentiation* **18**, 1241–1246.
- Dutilleul C., Garmier M., Noctor G., Mathieu C., Chétrit P., Foyer C.H. & De Paepe R. (2003) Leaf mitochondria modulate whole cell redox homeostasis, set antioxidant capacity, and determine stress resistance through altered signaling and diurnal regulation. *The Plant Cell* **15**, 1212–1226.
- Ederli L., Morettini R., Borgogni A., Wasternack C., Miersch O., Reale L., Ferranti F., Tosti N. & Pasqualini S. (2006) Interaction between nitric oxide and ethylene in the induction of alternative oxidase in ozone-treated tobacco plants. *Plant Physiology* **142**, 595–608.
- Epple P., Mack A.A., Morris V.R.F. & Dangl J.L. (2003) Antagonistic control of oxidative stress-induced cell death in *Arabidopsis* by two related, plant-specific zinc finger proteins. *Proceedings of the National Academy of Sciences of the United States of America* **100**, 6831–6836.
- Eulgem T. (2005) Regulation of the *Arabidopsis* defense transcriptome. *Trends in Plant Science* **10**, 71–78.
- Fath A., Bethke P.C. & Jones R.L. (2001) Enzymes that scavenge reactive oxygen species are down-regulated prior to gibberellic acid-induced programmed cell death in barley aleurone. *Plant Physiology* **126**, 156–166.
- Finnegan P.M., Soole K.L. & Umbach A.L. (2004) Alternative mitochondrial electron transport proteins in plants. In *Plant Mitochondria: From Genome to Function* (eds D.A. Day, A.H. Millar & J. Whelan) pp. 163–230. Kluwer Academic Publishers, Dordrecht, The Netherlands.
- Foyer C.H. & Noctor G. (2005) Redox homeostasis and antioxidant signaling: a metabolic interface between stress perception and physiological responses. *The Plant Cell* **17**, 1866–1875.
- Garmier M., Priault P., Vidal G., Driscoll S., Djebbar R., Boccarda M., Mathieu C., Foyer C.H. & De Paepe R. (2007) Light and oxygen are not required for harpin-induced cell death. *Journal of Biological Chemistry* **282**, 37556–37566.
- Gaupels F., Spiazzi-Vandelle E., Yang D. & Delledonne M. (2011) Detection of peroxynitrite accumulation in *Arabidopsis thaliana* during the hypersensitive defense response. *Nitric Oxide* **25**, 222–228.
- Gopalan S., Wei W. & He S.Y. (1996) *hrp* gene-dependent induction of *hin1*: a plant gene activated rapidly by both harpins and the *avrPto* gene-mediated signal. *The Plant Journal* **10**, 591–600.
- Halliwell B. (2003) Oxidative stress in cell culture: an under-appreciated problem? *FEBS Letters* **540**, 3–6.
- Heath M.C. (2000) Hypersensitive response-related death. *Plant Molecular Biology* **44**, 321–334.
- Ho L.H.M., Giraud E., Uggalla V., Lister R., Clifton R., Glen A., Thirkettle-Watts D., Van Aken O. & Whelan J. (2008) Identification of regulatory pathways controlling gene expression of stress-responsive mitochondrial proteins in *Arabidopsis*. *Plant Physiology* **147**, 1858–1873.
- Huang X., von-Rad U. & Durner J. (2002) Nitric oxide induces transcriptional activation of the nitric oxide-tolerant alternative oxidase in *Arabidopsis* suspension cells. *Planta* **215**, 914–923.
- Jiang Z.-Y., Woollard A.C.S. & Wolff S.P. (1990) Hydrogen peroxide production during experimental protein glycation. *FEBS Letters* **268**, 69–71.
- Kiba A., Lee K.Y., Ohnishi K. & Hikichi Y. (2008) Comparative expression analysis of genes induced during development of bacterial rot and induction of hypersensitive cell death in lettuce. *Journal of Plant Physiology* **165**, 1757–1773.
- Kiba A., Lee K.Y., Ohnishi K., Park P., Nakayashiki H., Tosa Y., Mayama S. & Hikichi Y. (2009) Induction of reactive oxygen generation and functional changes in mitochondria and their involvement in the development of bacterial rot in lettuce caused by *Pseudomonas cichorii*. *Physiological and Molecular Plant Pathology* **74**, 45–54.
- King E.O., Ward M.K. & Raney D.E. (1954) Two simple media for the demonstration of pyocyanin and fluorescin. *Journal of Laboratory and Clinical Medicine* **44**, 301–307.
- Kliebenstein D.J., Dietrich R.A., Martin A.C., Last R.L. & Dangl J.L. (1999) LSD1 regulates salicylic acid induction of copper zinc superoxide dismutase in *Arabidopsis thaliana*. *Molecular Plant-Microbe Interactions* **12**, 1022–1026.
- Krause M. & Durner J. (2004) Harpin inactivates mitochondria in *Arabidopsis* suspension cells. *Molecular Plant-Microbe Interactions* **17**, 131–139.
- Lacomme C. & Roby D. (1999) Identification of early marker genes of the hypersensitive response in *Arabidopsis thaliana*. *FEBS Letters* **459**, 149–153.
- Lam E., Kato N. & Lawton M. (2001) Programmed cell death, mitochondria and the plant hypersensitive response. *Nature* **411**, 848–853.

- Leitner M., Vandelle E., Gaupels F., Bellin D. & Delledonne M. (2009) NO signals in the haze. Nitric oxide signaling in plant defense. *Current Opinion in Plant Biology* **12**, 451–458.
- Li Z. & Xing D. (2011) Mechanistic study of mitochondria-dependent programmed cell death induced by aluminum phytotoxicity using fluorescence techniques. *Journal of Experimental Botany* **62**, 331–343.
- Lin R.C., Ding Z.S., Li L.B. & Kuang T.Y. (2001) A rapid and efficient DNA miniprep suitable for screening transgenic plants. *Plant Molecular Biology Reporter* **19**, 379a–379e.
- van Loon L.C., Geraats B.P.J. & Linthorst H.J.M. (2006) Ethylene as a modulator of disease resistance in plants. *Trends in Plant Science* **11**, 184–191.
- Maxwell D.P., Wang Y. & McIntosh L. (1999) The alternative oxidase lowers mitochondrial reactive oxygen production in plant cells. *Proceedings of the National Academy of Sciences of the United States of America* **96**, 8271–8276.
- Maxwell D.P., Nickels R. & McIntosh L. (2002) Evidence of mitochondrial involvement in the transduction of signals required for the induction of genes associated with pathogen attack and senescence. *The Plant Journal* **29**, 269–279.
- Mazel A. & Levine A. (2001) Induction of cell death in *Arabidopsis* by superoxide in combination with salicylic acid or with protein synthesis inhibitors. *Free Radical Biology and Medicine* **30**, 98–106.
- Millar A.H. & Day D.A. (1996) Nitric oxide inhibits the cytochrome oxidase but not the alternative oxidase of plant mitochondria. *FEBS Letters* **398**, 155–158.
- Mittler R., Vanderauwera S., Suzuki N., Miller G., Tognetti V.B., Vandepoele K., Gollery M., Shulaev V. & Van Breusegem F. (2011) ROS signaling: the new wave? *Trends in Plant Science* **16**, 300–309.
- Møller I.M. (2001) Plant mitochondria and oxidative stress: electron transport, NADPH turnover, and metabolism of reactive oxygen species. *Annual Review of Plant Physiology and Plant Molecular Biology* **52**, 561–591.
- Mosher S., Moeder W., Nishimura N., Jikumaru Y., Joo S.-H., Urquhart W., Klessig D.F., Kim S.-K., Nambara E. & Yoshioka K. (2010) The lesion-mimic mutant *cpr22* shows alterations in abscisic acid signaling and abscisic acid insensitivity in a salicylic acid-dependent manner. *Plant Physiology* **152**, 1901–1913.
- Mur L.A.J., Kenton P. & Draper J. (2005) *In planta* measurements of oxidative bursts elicited by avirulent and virulent bacterial pathogens suggests that H₂O₂ is insufficient to elicit cell death in tobacco. *Plant, Cell and Environment* **28**, 548–561.
- Mur L.A.J., Laarhoven L., Harren F.J.M., Hall M.A. & Smith A.R. (2008) Nitric oxide interacts with salicylate to regulate biphasic ethylene production during the hypersensitive response. *Plant Physiology* **148**, 1537–1546.
- Murphy M.E. & Noack E. (1994) Nitric oxide assay using haemoglobin method. *Methods in Enzymology* **233**, 240–250.
- Mysore K.S. & Ryu C.-M. (2004) Nonhost resistance: how much do we know? *Trends in Plant Science* **9**, 97–104.
- Noctor G., De Paepre R. & Foyer C.H. (2007) Mitochondrial redox biology and homeostasis in plants. *Trends in Plant Science* **12**, 125–134.
- Nomura K., Melotto M. & He S.-Y. (2005) Suppression of host defense in compatible plant–*Pseudomonas syringae* interactions. *Current Opinion in Plant Biology* **8**, 361–368.
- Norman C., Howell K.A., Millar A.H., Whelan J.M. & Day D.A. (2004) Salicylic acid is an uncoupler and inhibitor of mitochondrial electron transport. *Plant Physiology* **134**, 492–501.
- Ordog S.H., Higgins V.J. & Vanlerberghe G.C. (2002) Alternative oxidase is not a critical component of plant viral resistance but may play a role in the hypersensitive response. *Plant Physiology* **129**, 1858–1865.
- Pontier D., Godiard L., Marco Y. & Roby D. (1994) *hsr203J*, a tobacco gene whose activation is rapid, highly localized and specific for incompatible plant/pathogen interactions. *The Plant Journal* **5**, 507–521.
- Purvis A.C. (1997) Role of the alternative oxidase in limiting superoxide production by plant mitochondria. *Physiologia Plantarum* **100**, 165–170.
- Qin G., Meng X., Wang Q. & Tian S. (2009) Oxidative damage of mitochondrial proteins contributes to fruit senescence: a redox proteomics analysis. *Journal of Proteome Research* **8**, 2449–2462.
- Rhoads D.M. & McIntosh L. (1992) Salicylic acid regulation of respiration in higher plants: alternative oxidase expression. *The Plant Cell* **4**, 1131–1139.
- Robinson K.M., Janes M.S. & Beckman J.S. (2008) The selective detection of mitochondrial superoxide by live cell imaging. *Nature Protocols* **3**, 941–947.
- Robson C.A. & Vanlerberghe G.C. (2002) Transgenic plant cells lacking mitochondrial alternative oxidase have increased susceptibility to mitochondria-dependent and -independent pathways of programmed cell death. *Plant Physiology* **129**, 1908–1920.
- Robson C.A., Zhao D.Y. & Vanlerberghe G.C. (2008) Interactions between mitochondrial electron transport, reactive oxygen species, and the susceptibility of *Nicotiana tabacum* cells to programmed cell death. *Botany* **86**, 278–290.
- Sambrook J. & Russell D.W. (2001) *Molecular Cloning: A Laboratory Manual*. Cold Spring Harbor Laboratory Press, Cold Spring Harbor, NY, USA.
- Sieger S.M., Kristensen B.K., Robson C.A., Amirsadeghi S., Eng E.W.Y., Abdel-Mesih A., Møller I.M. & Vanlerberghe G.C. (2005) The role of alternative oxidase in modulating carbon use efficiency and growth during macronutrient stress in tobacco cells. *Journal of Experimental Botany* **56**, 1499–1515.
- Simons B.H., Millenaar F.F., Mulder L., van Loon L.C. & Lambers H. (1999) Enhanced expression and activation of alternative oxidase during infection of *Arabidopsis* with *Pseudomonas syringae* pv tomato. *Plant Physiology* **120**, 529–538.
- de Souza W.R., Vesecchi R., Dorta D.J., Uyemura S.A., Curti C. & Vargas-Rechia C.G. (2011) Characterization of *Rubus fruticosus* mitochondria and salicylic acid inhibition of reactive oxygen species generation at Complex III/Q cycle: potential implications for hypersensitive response of plants. *Journal of Bioenergetics and Biomembranes* **43**, 237–246.
- Spoel S.H. & Loake G.J. (2011) Redox-based protein modifications: the missing link in plant immune signaling. *Current Opinion in Plant Biology* **14**, 358–364.
- Sugie A., Murai K. & Takumi S. (2007) Alteration of respiration capacity and transcript accumulation level of alternative oxidase genes in necrosis lines of common wheat. *Genes and Genetic Systems* **82**, 231–239.
- Swidzinski J.A., Sweetlove L.J. & Leaver C.J. (2002) A custom microarray of gene expression during programmed cell death in *Arabidopsis thaliana*. *The Plant Journal* **30**, 431–446.
- Takahashi Y., Uehara Y., Berberich T., Ito A., Saitoh H., Miyazaki A., Terauchi R. & Kusano T. (2004) A subset of hypersensitive response marker genes, including *HSR203J*, is the downstream target of a spermine signal transduction pathway in tobacco. *The Plant Journal* **40**, 586–595.
- Tiwari B.S., Belenghi B. & Levine A. (2002) Oxidative stress increased respiration and generation of reactive oxygen species, resulting in ATP depletion, opening of mitochondrial permeability transition, and programmed cell death. *Plant Physiology* **128**, 1271–1281.
- Torres M.A., Jones J.D.G. & Dangl J.L. (2006) Reactive oxygen species signaling in response to pathogens. *Plant Physiology* **141**, 373–378.

- Van Der Straeten D., Chaerle L., Sharkov G., Lambers H. & Van Montagu M. (1995) Salicylic acid enhances the activity of the alternative pathway of respiration in tobacco leaves and induces thermogenicity. *Planta* **196**, 412–419.
- Vanlerberghe G.C. & McIntosh L. (1996) Signals regulating the expression of the nuclear gene encoding alternative oxidase of plant mitochondria. *Plant Physiology* **111**, 589–595.
- Vanlerberghe G.C., Day D.A., Wiskich J.T., Vanlerberghe A.E. & McIntosh L. (1995) Alternative oxidase activity in tobacco leaf mitochondria. Dependence on tricarboxylic acid cycle-mediated redox regulation and pyruvate activation. *Plant Physiology* **109**, 353–361.
- Vanlerberghe G.C., Yip J.Y.H. & Parsons H.L. (1999) In organello and *in vivo* evidence of the importance of the regulatory sulfhydryl/disulfide system and pyruvate for alternative oxidase activity in tobacco. *Plant Physiology* **121**, 793–803.
- Vanlerberghe G.C., Cvetkovska M. & Wang J. (2009) Is the maintenance of homeostatic mitochondrial signaling during stress a physiological role for alternative oxidase? *Physiologia Plantarum* **137**, 392–406.
- Vidal G., Ribas-Carbo M., Garmier M., Dubertret G., Rasmusson A.G., Mathieu C., Foyer C.H. & De Paep R. (2007) Lack of respiratory chain complex I impairs alternative oxidase engagement and modulates redox signaling during elicitor-induced cell death in tobacco. *The Plant Cell* **19**, 640–655.
- Vlot A.C., Dempsey D.A. & Klessig D.F. (2009) Salicylic acid, a multifaceted hormone to combat disease. *Annual Review of Phytopathology* **47**, 177–206.
- Weir I.E., Pham N.-A. & Hedley D.W. (2003) Oxidative stress is generated via the mitochondrial respiratory chain during plant cell apoptosis. *Cytometry* **54A**, 109–117.
- Winger A.M., Millar A.H. & Day D.A. (2005) Sensitivity of plant mitochondrial terminal oxidases to the lipid peroxidation product 4-hydroxy-2-nonenal (HNE). *Biochemical Journal* **387**, 865–870.
- Yao N., Tada Y., Sakamoto M., Nakayashiki H., Park P., Tosa Y. & Mayama S. (2002) Mitochondrial oxidative burst involved in apoptotic response in oats. *The Plant Journal* **30**, 567–579.
- Yao N., Eisfelder B.J., Marvin J. & Greenberg J.T. (2004) The mitochondrion – an organelle commonly involved in programmed cell death in *Arabidopsis thaliana*. *The Plant Journal* **40**, 596–610.
- Yun B.-W., Feechan A., Yin M., *et al.* (2011) S-nitrosylation of NADPH oxidase regulates cell death in plant immunity. *Nature* **478**, 264–268.

Received 26 October 2011; received in revised form 19 December 2011; accepted for publication 20 December 2011

SUPPORTING INFORMATION

Additional Supporting Information may be found in the online version of this article:

Figure S1. Diurnal changes in the level of *Aox1a* and *PAL* transcript in tobacco leaf either left untreated or mock-inoculated with H₂O.

Figure S2. Representative Northern blot showing level of *Aox1a* transcript in tobacco leaf at different times post-inoculation with pathovars of *P. syringae* or after mock-inoculation with H₂O.

Figure S3. Level of *Aox1a* transcript in *Arabidopsis* rosette leaves at different times post-inoculation with strains of *P. syringae* pv. *tomato* or after mock-inoculation with MgCl₂.

Table S1. Primer sequences used for RT-PCR.

Please note: Wiley-Blackwell are not responsible for the content or functionality of any supporting materials supplied by the authors. Any queries (other than missing material) should be directed to the corresponding author for the article.